Functional Connectivity Suggests Mean Pathway Radial Diffusivity as a Robust Metric of Anatomic Connectivity

Mark J Lowe[1], Ken E Sakaie[1], Katherine Koenig[1], Lael Stone[2], Robert Bermel[2], and Micheal D Phillips[1]

[1]*Imaging Institute, Cleveland Clinic, Cleveland, OH, United States,* [2]*Neurologic Institute, Cleveland Clinic, Cleveland, OH, United States*

Target Audience: Researchers interested in measuring diffusion based anatomic connectivity in a manner that easily permits comparison across studies.

Introduction: It has been shown by several studies that anatomic connectivity, as assessed by DTI, and resting state functional connectivity are related [1-3]. Although methods to assess functional connectivity are relatively standardized in the field, there are many diffusion-derived metrics for assessing anatomic connectivity between two brain regions[4]. We previously showed that using mean radial diffusivity, measured along a probabilistically tracked pathway between two brain regions, is highly correlated to resting state functional connectivity in multiple sclerosis(MS)[1]. This makes sense in the context that it is known that radial diffusivity is sensitive to myelination of white matter and this is often compromised in MS. We demonstrate here that mean pathway radial diffusivity (<RD>) in healthy controls has a similar correlation to resting state functional connectivity as in MS. Since most of the tissue microstructural properties that restrict radial diffusivity also improve neuronal conduction (axonal density, myelination, etc.), we suggest that <RD> is a robust, easily derived metric of anatomic connectivity in the human brain.

Methods: We acquired whole-brain RS-fMRI data and whole-brain HARDI data in 16 RR-MS patients and 19 age and gender matched control subjects.

Data acquisition. All data were acquired on a Siemens TIM Trio 3T MRI scanner (Erlangen, Germany) using a 12-channel receive-only head array. HARDI data were acquired with a twice-refocused spin echo[5] (TE/TR=102/7700msec, 128x128x48 matrix, FOV=256x256x96mm), 71 b=1000 sec/mm^2 acquisitions with gradient directions selected by a coulomb repulsion algorithm[6], and 8 b=0 acquisitions at equally spaced intervals. Motion correction was performed using FSL[7]. Resting state scan: Whole brain LFBF fMRI study: One hundred thirty two repetitions of 31-4mm thick axial slices acquired with TE/TR=29ms/2800 ms, 128x128 matrix, 256mm x 256mm FOV, receive bandwidth=1954Hz/pixel. The subject is instructed to rest with eyes closed and refrain from any voluntary motion.

Data analysis

Except for seed region definition, the analysis proceeded as described in reference [1]. We measure anatomic and functional connectivity in the transcallosal motor pathway (SMC), right hemisphere posterior cingulate-hippocampal pathway (RH PCC-AMTL), and left hemisphere posterior cingulate-hippocampal pathway (LH PCC-AMTL) in all 35 subjects.

Seed region definition

Seed regions for the SMC pathway are defined as the 9-voxel in-plane region centered on the maximum activated voxel in a finger tapping fMRI study performed in the same scan session. We define the seed region in each of the right and left hemisphere PCC by selecting a finite region in each hemisphere proximal to retrosplenial cortex, consistent with the Talairach locations reported in reference [8] . Using InstaCorr from the AFNI suite, we find the voxel within this region, for each hemisphere, that has high correlation to a region in posterior part of the ipsilateral hippocampus. Seeds were defined in all patients such that a similar network pattern was identified in all 35 subjects in the cross sectional study. The final PCC seed that resulted in robust connection to posterior hippocampus was taken as the center voxel of a 9 voxel seed. The hippocampal seed was taken as the centroid of the hippocampal region with high connectivity to the PCC voxel, as evidenced by InstaCorr. The method was validated as being robust in a 5 subject test-retest study.

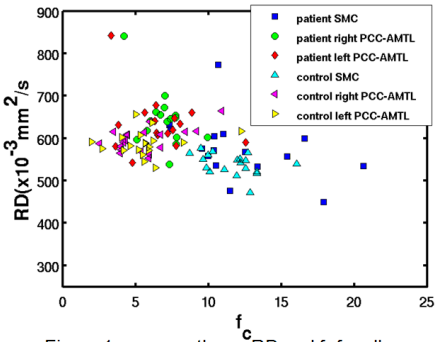

Figure 1: mean pathway RD and f_c for all assessed pathways in patients and controls

Fiber tracking

Using the seed and target regions defined above, probabilistic fiber tracking is performed on each study. The fiber tracking is described in detail in reference [1].

SD was performed with regularization by optimized by generalized cross validation[9]. Probabilistic fiber tracking was performed by rejection-sampling [10] using the above seed voxels. **Our tracking methodology has been demonstrated to be insensitive to the presence of MS lesions [11].**

Pathway dependent diffusion measures are calculated using the track density map, the scalar diffusion values, and a white matter mask constructed by segmenting scan 1 above using the FAST algorithm from the FSL library (7). Each measure <D> is calculated according to:

$$\langle D \rangle = \frac{\sum_T \sum_v D(v) \cdot w(v) \cdot WM(v)}{\sum_T \sum_v w(v) \cdot WM(v)} \qquad \text{Eq. 1}$$

where the D(v) is the particular tensor-based value of interest (e.g. FA) at voxel v and w(v) is a so-called track visitation map, in which the value of each voxel equals the number tracks generated by the probabilistic tractography algorithm that intersect that voxel. WM is a mask that is set to one for voxels determined to be mostly white matter from the FAST segmentation. An artifact of the track visitation map is that a large, spatially diffuse set of voxels are visited by a small number of tracks. A threshold approach was implemented using a histogram of nonzero values in the track visitation map. A bimodal distribution was found for each study, with a cutoff consistently found at the second bin. Values in the track visitation map, w(v), below this threshold were set to zero (see Fig 3 for a thresholded PCC-AMTL track map for a typical subject). The result is <FA>,<MD>,<AD>, and <RD> for every subject

Functional connectivity

The RS-fMRI metric, f_c, is calculated in the following manner: Right and left hemisphere SMC, hippocampal and PCC ROI's are defined using method described above. A reference timeseries is calculated from the arithmetic average of the nine pixels centered on the seed voxel. The cross correlation is calculated between r/l hemisphere SMC, RH PCC and AMTL, and LH PCC and AMTL. The result is a correlation for each of the three pathways. The cross correlation is converted to a Student t. This is taken to be f_c.

Results

f_c and <RD> significantly inversely correlate in

- Patients: SMC ($p<0.04$), PCC-AMTL right hemisphere ($p<0.01$)
- Controls: SMC($p<0.04$)
- Combining all pathways in patients, f_c and <RD> significantly inversely correlated: r=-0.54, $p<4\times10^{-5}$
- Combining all pathways in controls, f_c and <RD> significantly inversely correlated: r=-0.50, $p<4\times10^{-5}$
- Combining all pathways, all subjects, f_c and <RD> significantly inversely correlated (**note: 105 independent measures**—see Fig 1): r=-0.41, $p<5\times10^{-6}$

Discussion

All physiologic parameters of axons known to affect RD, mainly myelination and compactness of fibers, also affect conduction efficiency. Reduced myelination and/or reduced compactness will result in both higher radial diffusivity of water and reduced conduction efficiency. We show here that <RD> in three independent, directly connected functional pathways, is significantly inversely correlated to functional connectivity in healthy controls and that this correlation was approximately the same as in a population of age and gender-matched MS patients. This strongly suggests that <RD> is a robust measure of the degree of anatomic connectivity.

Acknowledgements

This study was made possible by a grant from the National Multiple Sclerosis Society.

References

[1] Lowe et al., HBM 29: 818-27 (2008)[2] Skudlarski et al., NeuroImage, 43: 554-61,(2008)[3] Van Den Heuvel, HBM (2009)[4] Jones et al., NeuroImage (2012) [5] Reese TG et al Magn Reson Med 49:177-82(2003)[6] Jones DK et al Magn Reson Med 42:515-25(1999)[7] Smith SM et al Neuroimage 23 Suppl 1:S208-19(2004)[8] Greicius, MD et al., PNAS **100**, 253-8, (2003)[9] Sakaie KE et al., Neuroimage 34:169-76(2007)[10] Tournier JD et al ISMRM 13:1343(2005)[11] Pines et al., ISMRM :17: 633(2009)